Journal of Luminescence 210 (2019) 169–174

Contents lists available at ScienceDirect

Journal of Luminescence

journal homepage: www.elsevier.com/locate/jlumin

Comparison of 10 MeV electron beam radiation effect on InGaN/GaN and GaN/AlGaN multiple quantum wells

Qingxuan Li[a], Bo Li[b], Lei Wang[b,*], Zhongming Zheng[a], Baoping Zhang[a,*], Ningyang Liu[c,*], Binhong Li[b], Mengxin Liu[b], Yang Huang[b], Zheng Gong[c], Zhitao Chen[c], Xinyu Liu[b,d], Jiajun Luo[b,d], Zhengsheng Han[b,d]

[a] Laboratory of Micro/Nano-Optoelectronics, and the Department of Electronic Engineering, College of Electronic Science and Technology, Xiamen University, Xiamen, Fujian 361005, China
[b] Key Laboratory of Silicon Device Technology, and the Institute of Microelectronics, Chinese Academy of Sciences, Beijing 100029, China
[c] Guangdong Institute of Semiconductor Industrial Technology, Guangzhou, Guangdong 510650, China
[d] University of Chinese Academy of Sciences, Beijing 100049, China

ARTICLE INFO

Keywords:
InGaN/GaN
GaN/AlGaN
Radiation effect
Non-radiation recombination centers
Exciton localization energy
Internal quantum efficiency

ABSTRACT

Radiation effects of 10 MeV electrons on blue-lighting InGaN/GaN multiple quantum wells (MQWs) and ultraviolet-lighting GaN/AlGaN MQWs were investigated and compared by means of temperature-dependent and time-resolved photoluminescence (PL) methods. It was found that GaN/AlGaN MQWs showed better radiation tolerance than InGaN/GaN MQWs. In detail, the internal quantum efficiency of InGaN/GaN MQWs decreased sharply with increasing electron irradiation fluence whereas that of GaN/AlGaN MQWs remained nearly constant. The degradation of the emission properties of InGaN/GaN MQWs after irradiation was attributed to the generation of non-radiation recombination centers (NRCs) in MQWs. On the other hand, the radiation hardness of GaN/AlGaN MQWs was proved to be related to two factors: the irradiation-induced reduction of both exciton localization energy and NRC density. The results reported here are significant for the evaluation and design of GaN-based optoelectronic and electronic devices used in radiation environments.

1. Introduction

III-nitrides have been attracting much attention since their potential applications in optoelectronic devices, high frequency and high power electronic devices due to the excellent physical and chemical properties [1–4]. The III-nitrides show excellent light luminescence and electron transport properties in spite of lattice and thermal mismatch with substrates such as sapphire, silicon and silicon carbide. Most optoelectronic devices based on III-nitrides are designed using InGaN/GaN or GaN/AlGaN multiple quantum wells (MQWs) [5–8]. Therefore, an in-depth understanding of the basic physical properties of the MQWs is of great importance. It has been reported that GaN is a better anti-radiation material than Si and GaAs due to its higher displacement energies under radiation environments, demonstrating their potential application in space and other severe radiative fields [9]. Due to the peculiar chemical activity of indium in InGaN alloy epitaxial layers, indium clusters in InGaN layers are widely observed and analyzed. In addition, most of InGaN-related devices show degradation with irradiation fluence of high energy particles. On the contrary, however, the performance of some AlGaN-related devices such as ultraviolet light emitting diodes and high electron mobility transistors are improved under certain extent of high energy particle irradiation [10,11]. Up to now, however, the irradiation-caused variation mechanisms of InGaN/GaN MQWs and GaN/AlGaN MQWs, as the most common low dimensional structures in III-nitride devices, have not been systematically analyzed and compared with the same radiation source and conditions.

The Van Allen radiation belt, surrounding the Earth in the near-surface cosmic space, is a radiation band full of high energy particles. It consists mainly of electrons with energy up to several MeV and protons with energy up to several hundred MeV captured in the geomagnetic field [12]. Therefore, in this work, 10 MeV electrons were chosen to study the irradiation effects. Temperature-dependent photoluminescence (TDPL) and time-resolved photoluminescence (TRPL) spectra were measured to reveal the difference of the variation mechanisms of InGaN/GaN and GaN/AlGaN MQWs. The internal quantum efficiency (IQE), composition-fluctuation caused localization, and density of non-radiative recombination centers (NRCs) were extracted simultaneously from TDPL and TDPL analyses. Radiation damage

* Corresponding authors.
E-mail addresses: wangle@ime.ac.cn (L. Wang), bzhang@xmu.edu.cn (B. Zhang), iamlpo@126.com (N. Liu).

https://doi.org/10.1016/j.jlumin.2019.02.034
Received 14 December 2018; Received in revised form 14 February 2019; Accepted 15 February 2019
Available online 16 February 2019
0022-2313/

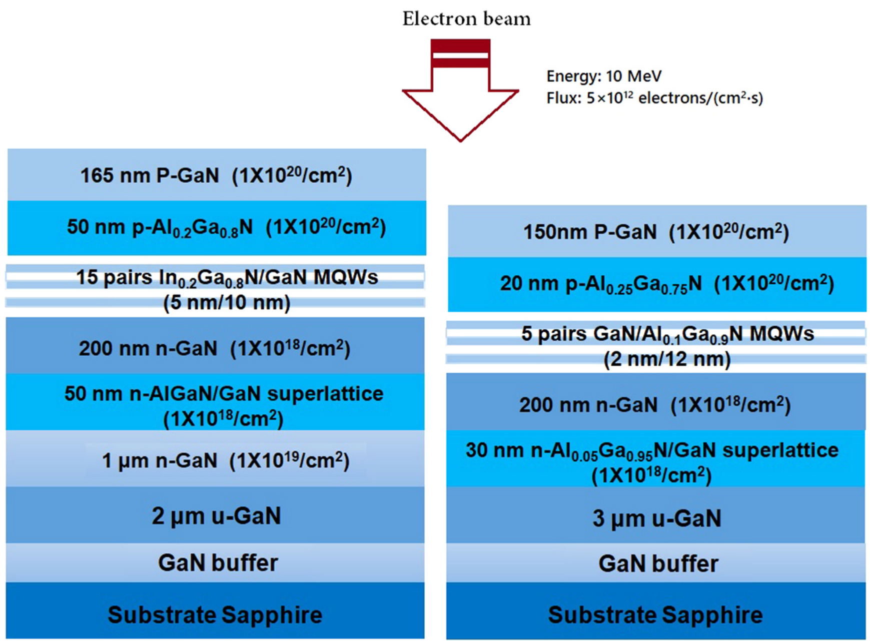

Fig. 1. Schematic diagrams of InGaN/GaN and GaN/AlGaN MQWs structures with electron beam irradiation.

coefficient of 10 MeV electrons on GaN-based epitaxial layers was obtained from TRPL spectra.

2. Material and methods

The sample structures were shown in Fig. 1. The epitaxial growth of InGaN/GaN and GaN/AlGaN MQWs wafers were performed by metal organic chemical vapor deposition (MOCVD) on c-plane (0001) sapphire. For InGaN/GaN MQWs wafer, the layers include GaN buffer layer, 2 μm u-GaN and 1 μm n-type GaN layers, 50 nm n-type GaN/AlGaN super-lattice, 200 nm n-type GaN layer, fifteen periods of InGaN/GaN MQWs in which indium composition was 0.2, 50 nm p-type AlGaN layer and 165 nm p-type GaN capping layer. The thicknesses of InGaN wells and GaN barriers were 5 nm and 10 nm, respectively. Analogously, the GaN/AlGaN MQWs wafer is composed of GaN buffer layer, 3 μm u-GaN layer, 30 nm n-type GaN/AlGaN super-lattice, 200 nm n-type GaN layer, five periods of GaN/AlGaN MQWs in which aluminum composition was 0.1, 20 nm p-type AlGaN layer and 150 nm p-type GaN capping layer. The thicknesses of GaN wells and AlGaN barriers were 2 nm and 12 nm, respectively.

The10 MeV electron beam irradiation experiments were carried out on a linear electron accelerator with a degree of instability less than 5%. The electron beam fluence splits were set as5×10^{14} e/cm^2 and 1×10^{15} e/cm^2 with electron flux of 5×10^{12} e/(cm^2·s). To avoid the heating effect, irradiation time was set to be 20 s each time with an interval of 600 s. Before and after the irradiation, TDPL spectra were measured by iHR550 (HORIBA JobinYvon) PL system from 10 to 300 K (10, 20, 40, 60, 80, 120, 200 and 300 K) under excitation of a 325 nm He-Cd laser. TRPL measurements were carried out in FLS980 for InGaN/GaN MQWs with an excitation laser of 375 nm and Life spec-II for GaN/AlGaN MQWs with an excitation laser of 280 nm (both are Edinburgh Instruments) at room temperature.

3. Results and discussion

3.1. Optical properties measured by room temperature PL

In order to compare the nature of microscopic mechanisms, room temperature PL spectra of InGaN/GaN and GaN/AlGaN MQWs was measured before and after irradiation, and the results were shown in Fig. 2. In InGaN/GaN MQWs, only the PL peak from MQWs could be seen, whereas both MQWs' PL peak and yellow band luminescence (YBL) peak were observed in GaN/AlGaN MQWs. The existence of YBL in GaN/AlGaN MQWs indicates a large number of defects in the lattice introduced during the growth process. The PL intensity of InGaN/GaN MQWs gradually decreased with increasing electron beam fluence. However, the PL intensity of GaN/AlGaN MQWs and YBL firstly

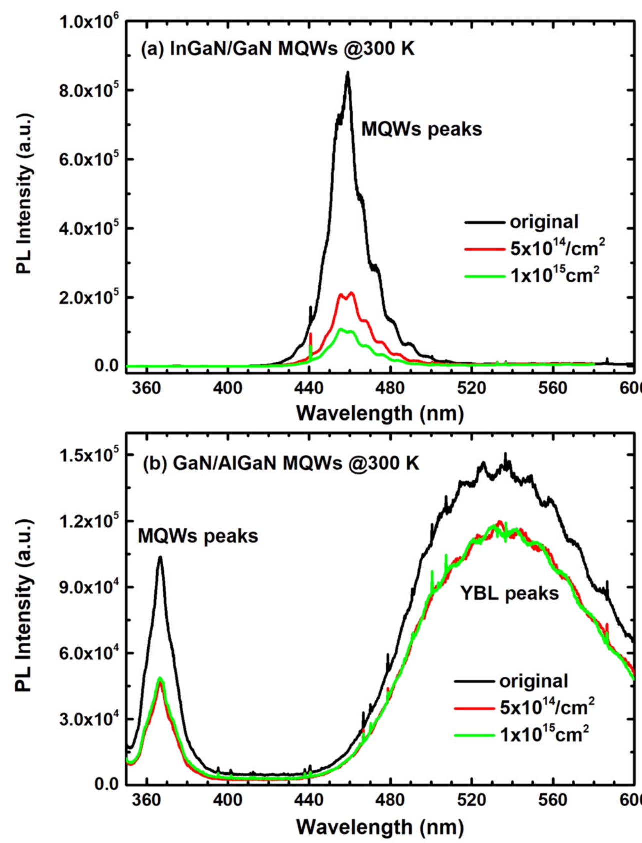

Fig. 2. Room temperature PL spectra of (a) InGaN/GaN and (b) GaN/AlGaN MQWs at different electron fluence.

Table 1
PL Peak and FWHMs of InGaN/GaN MQWs.

	Fluence (e/cm^2)	Original	5 × 10^{14}	1 × 10^{15}
MQWs	PL peak (nm)	458.19	459.48	458.71
	FWHM (nm)	17.92	18.6	18.34

decreased when electron beam fluence reached 5×10^{14} e/cm^2 and then remained nearly constant up to a fluence of 1×10^{15} e/cm^2.

The above results indicate that, the electron beam irradiation in this study gives negative effects on the optical properties of both InGaN/GaN and GaN/AlGaN MQWs, as well as the defects-related YBL. InGaN/GaN MQWs were found to be more sensitive to electron irradiation than GaN/AlGaN MQWs, which provides a great evidence that GaN/AlGaN MQWs are more resistant to electron irradiation damage than InGaN/GaN MQWs.

Based the analysis above, it can be concluded that the electron beam irradiation in this study gives negative effects on the light emissions of both InGaN/GaN and AlGaN/GaN MQWs, as well as defects-related YBL. Moreover, InGaN/GaN MQWs are more sensitive to electron irradiation than GaN/AlGaN MQWs. In the other words, GaN/AlGaN quantum wells are more resistant to electron irradiation than InGaN/GaN quantum wells.

Variations of PL peak positions and full width at half maximums (FWHM) of both InGaN/GaN and GaN/AlGaN MQWs as a function of electron fluence were also analyzed and the results are shown in Tables 1 and 2. Both the peak positions and FWHM of the MQWs and YBL remained nearly constant before and after irradiation, indicating that the variations of Quantum Confined Stark Effects do not occur in InGaN/GaN or GaN/AlGaN MQWs after the electron beam irradiation.

3.2. IQE, exciton localization energy, and density of NRCs obtained by TDPL

TDPL measurements were carried out to investigate the irradiation effects on the IQE, exciton localization, NRCs density, and the thermal activation energy related with the non-radiative recombination process in all InGaN/GaN and GaN/AlGaN MQWs samples, which are all critical factors for the light emitting properties of MQWs.

At low temperatures, the non-radiative recombination processes were nearly completely suppressed such that, the actual IQE of MQWs can be defined by the following formula [13]

$$\eta_{IQE} = \frac{I_{PL}(300K)}{I_{PL}(10K)} \tag{1}$$

where η_{IQE} is the IQE, $I_{PL}(300\,K)$ and $I_{PL}(10\,K)$ are the integrated PL intensities at 300 K and 10 K, respectively. The IQE values of both InGaN/GaN and GaN/AlGaN MQWs samples with different electron beam fluence are listed in Table 3 and 4. The initial IQE of InGaN/GaN MQWs is much larger than that of GaN/AlGaN MQWs probably due to the strong composition-fluctuation-caused localization effects in the former and more point-defects as NRCs in the latter. It is also clearly seen that the IQE of InGaN/GaN MQWs decreases gradually with increasing electron beam fluence whereas that of GaN/AlGaN MQWs remains nearly constant, meaning that, the light emission properties of InGaN/GaN MQWs are more sensitive to electron irradiation than GaN/AlGaN MQWs, which is consistent with the results obtained earlier from the room temperature PL spectra of InGaN/GaN and GaN/AlGaN MQWs.

Table 2
PL Peak and FWHMs of GaN/AlGaN MQWs.

	Fluence (e/cm^2)	Original	5 × 10^{14}	1 × 10^{15}
MQWs	PL peak (nm)	366.70	366.59	366.71
	FWHM (nm)	14.79	14.93	15.44
YBL	PL peak (nm)	537.76	539.03	538.43
	FWHM (nm)	103.28	98.46	97.48

Table 3
IQE, Active Energies (E_{A1} and E_{A2}) and Parameters (C_1 and C_2) in InGaN/GaN MQWs with Electron Fluence.

Fluence (e/cm^2)	η_{IQE}	E_{A1} (meV)	C_1	E_{A2} (meV)	C_2
Original	13.07%	3.80	2.28	30.50	12.73
5 × 10^{14}	3.72%	3.31	1.36	28.62	37.04
1 × 10^{15}	1.67%	3.53	1.33	22.20	43.28

Table 4
IQE, Active Energies (E_{A1} and E_{A2}) and Parameters (C_1 and C_2) in GaN/AlGaN MQWs with Electron Fluence.

Fluence (e/cm^2)	η_{IQE}	E_{A1} (meV)	C_1	E_{A2} (meV)	C_2
Original	0.32%	12.80	7.86	62.64	875.77
5 × 10^{14}	0.19%	5.64	2.37	32.36	188.40
1 × 10^{15}	0.39%	4.55	1.97	31.57	211.99

To further investigate the difference in irradiation-caused variation mechanisms between InGaN/GaN and GaN/AlGaN MQWs, the variations of exciton localization and NRCs density in MQWs with the electron beam fluence are derived from Arrhenius fitting plots of TDPL spectrums by the formula [13]

$$I_{TDPL}(T) = \left[1 + C_1 exp\left(-\frac{E_{A1}}{k_B T}\right) + C_2 exp\left(-\frac{E_{A2}}{k_B T}\right)\right]^{-1} \tag{2}$$

where $I_{TDPL}(T)$ is the normalized PL integrated intensity at temperature, T. C_1 and C_2 are parameters corresponding to densities of NRCs in MQWs. E_{A1} and E_{A2} are the activation energies related to the non-radiative recombination process. The small one, E_{A1}, can be attributed to the exciton localization energy, and the big one, E_{A2}, is considered as the potential barrier between the localized potential minima and the NRCs or dislocations inside the wells. k_B is the Boltzmann constant [13–15]. Fig. 3(a) and (b) show the Arrhenius plots of the integrated PL intensity obtained from the InGaN/GaN and GaN/AlGaN MQWs emission over the temperature range of 10–300 K, respectively. All the fitting parameters are also listed in Tables 3 and 4.

In InGaN/GaN MQWs, the E_{A1}, E_{A2}, and C_1 remained constant or decreased slightly with increasing electron fluence. However, C_2 increased more than three times when the electron beam fluence reached 1×10^{15} e/cm^2. The constant values of E_{A1} and E_{A2} indicate no obvious changes in indium-fluctuation-caused localization effects after irradiation, meanwhile, the increase of C_2 indicates the generation of new NRCs in MQWs layers after irradiation. Therefore, it can be concluded that the decrease of IQE in InGaN/GaN MQWs is mainly due to the increase of NRCs induced by the electron beam irradiation. The absence of variation of the indium localization effects in InGaN/GaN MQWs implies that, the 10 MeV electron beam irradiation does not lead to obvious thermal spike effect in InGaN QW layer, which is a different result from the 30 MeV silicon ion irradiation reported earlier [16].

In GaN/AlGaN MQWs, all the E_{A1}, E_{A2}, C_1 and C_2 parameters decreased with increasing electron fluence. In detail, the reductions of E_{A1} and E_{A2} means the less binding efficiency of carriers or excitons in MQWs which is negative to the radiative recombination probability. On the other hand, the reductions of C_1 and C_2 indicate the decrease of NRCs density in MQWs, indicating that the ionization state or point defect in GaN and AlGaN epitaxial layer was improved by electron beam irradiation. Therefore, the constant IQE of GaN/AlGaN MQWs is caused by the balance of the reduction of exciton localization energies and the decrease of NRCs densities.

To further illustrate the localization effects in InGaN/GaN and GaN/AlGaN MQWs, the exciton-phonon interaction obtained in PL spectra at

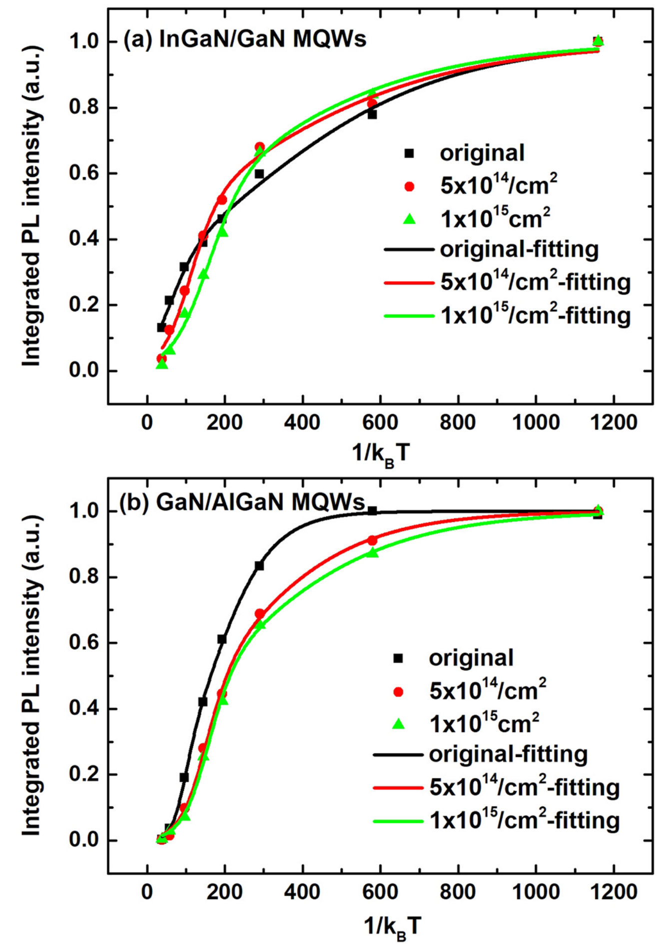

Fig. 3. Normalized integrated PL intensity with the Arrhenius fitting plots of (a) InGaN/GaN MQWs and (b) GaN/AlGaN MQWs with different electron fluence.

10 K was analyzed. The longitudinal optical (LO) phonon sidebands in the low temperature PL spectra (at 10 K) of the as-grown and the irradiated InGaN/GaN MQWs and GaN/AlGaN MQWs were fitted by a series of Gaussian curves after a linear subtraction of the background, as plotted in Figs. 4 and 5, respectively. In those plots, the LO phonon sidebands and their relative strength in the PL spectra were analyzed in term of the Huang-Rhys factor, S_n, given by the intensity ratio of the phonon sidebands [17]

$$S_n = (n+1)\frac{I_{n+1}}{I_n} \tag{3}$$

where I_n is the integrated intensity of the nLO phonon sidebands. For both samples, in order to improve the quality of MQWs, several pairs of MQWs were pre-grown, which relaxed the stress caused by lattice mismatch and improved the crystalline quality just like the buffer layer. Therefore, two sets of LO side bands can be seen from the fitting results of InGaN/GaN MQWs and GaN/AlGaN MQWs, respectively. However, in this work, the second set LO side bands (the purple short dash line) from the buffer-MQWs are not discussed.

Energy differences between the zero phonon line (ZPL) and 1LO peaks, 1LO and 2LO peaks in InGaN/GaN and GaN/AlGaN MQWs were estimated and the results were listed in Tables 5 and 6. The energy differences were between 86 and 94 meV. Therefore, 1LO and 2LO sidebands in the PL spectra at 10 K were confirmed to originate from one LO phonon-coupled and two LO phonons-coupled excitons in InGaN/GaN MQWs and GaN/AlGaN MQWs, respectively. The values of S_0, S_1 and the ratio S_1/S_0 before and after the irradiation are also listed in Tables 5 and 6. The localization of an exciton can cause strong

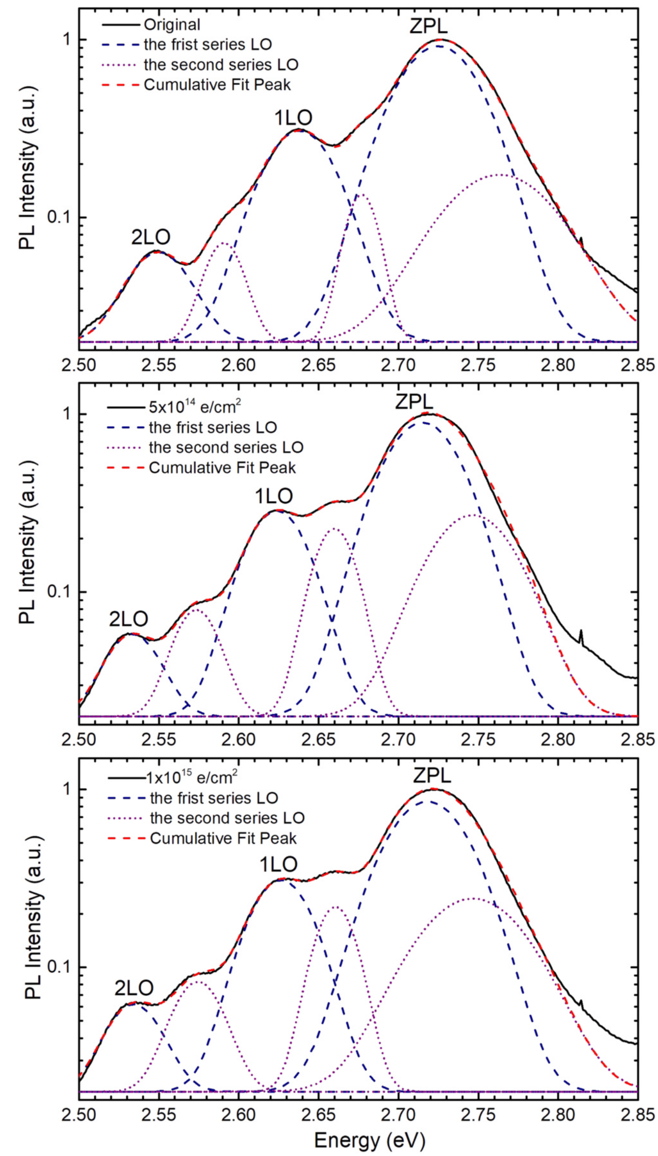

Fig. 4. PL spectra of the ZPL, 1LO and 2LO phonon sidebands at temperature of 10 K for InGaN/GaN MQWs with multi-Gaussian peaks fitting.

coupling with LO phonons [18]. Therefore, the intensity of the phonon sidebands tends to be greater for MQWs with strongly localized excitons. So the ratio S_1/S_0 should be an indicator of exciton localization [17,18].

For InGaN/GaN MQWs, before and after the electron beam irradiation, the ratio S_1/S_0 is basically a constant with increasing electron fluence; whereas for the GaN/AlGaN MQWs, the ratio S_1/S_0 decreases with increasing electron fluence. Therefore, it can be concluded that the exciton localization in InGaN/GaN MQWs remains unchanged, whereas that in GaN/AlGaN MQWs is weakened. This observation is consistent with the analysis of E_{A1} which is considered to be related to the exciton localization energy in MQWs.

In overall, the irradiation damage mechanisms of 10 MeV electron beam on the InGaN/GaN and GaN/AlGaN MQWs are completely different: (1) electron irradiation can increase the NRC density in InGaN/GaN MQWs but decrease the NRC density in GaN/AlGaN MQWs; (2) the exciton localization effect in InGaN/GaN MQWs keeps nearly constant but that in GaN/AlGaN MQWs is weakened; (3) the less sensitivity of GaN/AlGaN MQWs than InGaN/GaN MQWs to electron irradiation is mainly due to the comprehensive results of the above mentioned two points rather than simple irradiation hardness of AlGaN epitaxial layers.

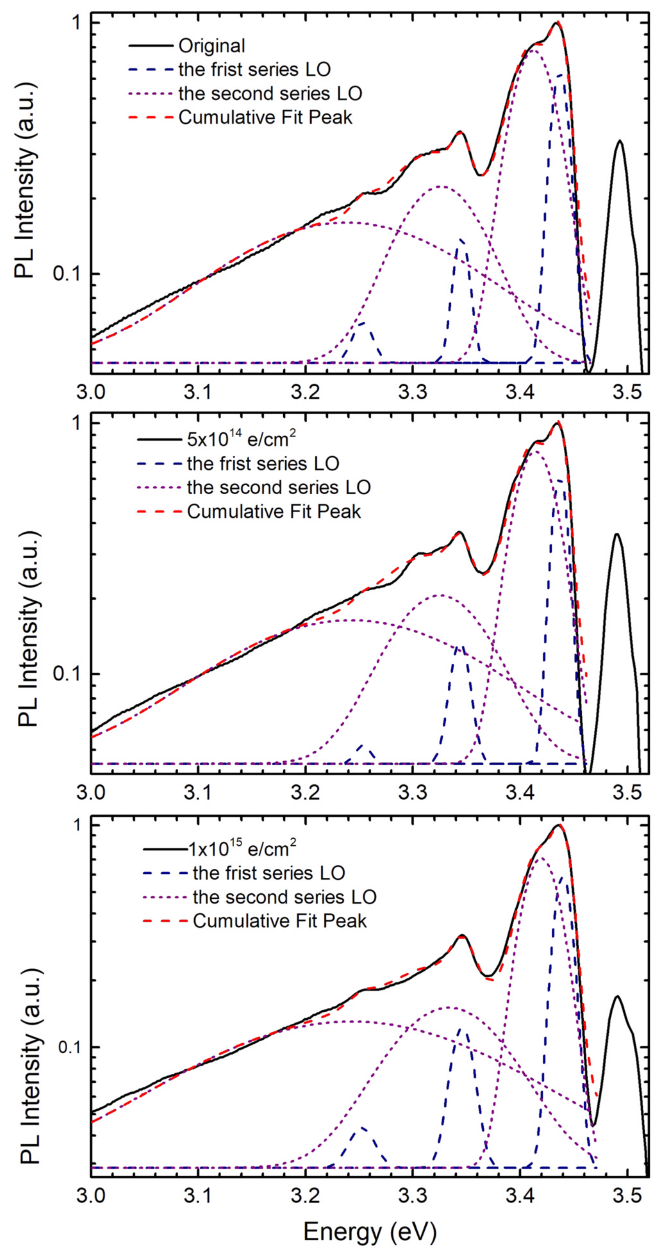

Fig. 5. PL spectra of the ZPL, 1LO and 2LO phonon sidebands at temperature of 10 K for GaN/AlGaN MQWs with multi-Gaussian peaks fitting.

Table 5
LO Phonon Energy and S_0/S_1 in InGaN/GaN MQWs with Different Electron Fluence.

Fluence (e/cm2)	Phonon energy (meV)		Huang-Rhys factor		
	1LO	2LO	S_0	S_1	S_1/S_0
Original	86.9	88.2	0.273	0.258	0.945
5×10^{14}	91.3	90.2	0.243	0.241	0.992
1×10^{15}	91.7	92.2	0.263	0.245	0.932

3.3. Carrier ultrafast dynamics and irradiation damage coefficient obtained by TRPL

Carrier non-radiative recombination lifetimes are critical parameters for the evaluation of non-radiative recombination process in MQWs at room temperature. The TRPL measurements were carried out to compare the difference of carrier ultrafast dynamics process between the InGaN/GaN and GaN/AlGaN MQWs.

Table 6
LO Phonon Energy and S_0/S_1 in GaN/AlGaN MQWs with Different Electron Fluence.

Fluence (e/cm^2)	Phonon energy (meV)		Huang-Rhys factor		
	1LO	2LO	S_0	S_1	S_1/S_0
Original	91.7	92.1	0.144	0.542	3.764
5×10^{14}	93.2	90.4	0.187	0.146	0.781
1×10^{15}	93.9	93.6	0.202	0.362	1.792

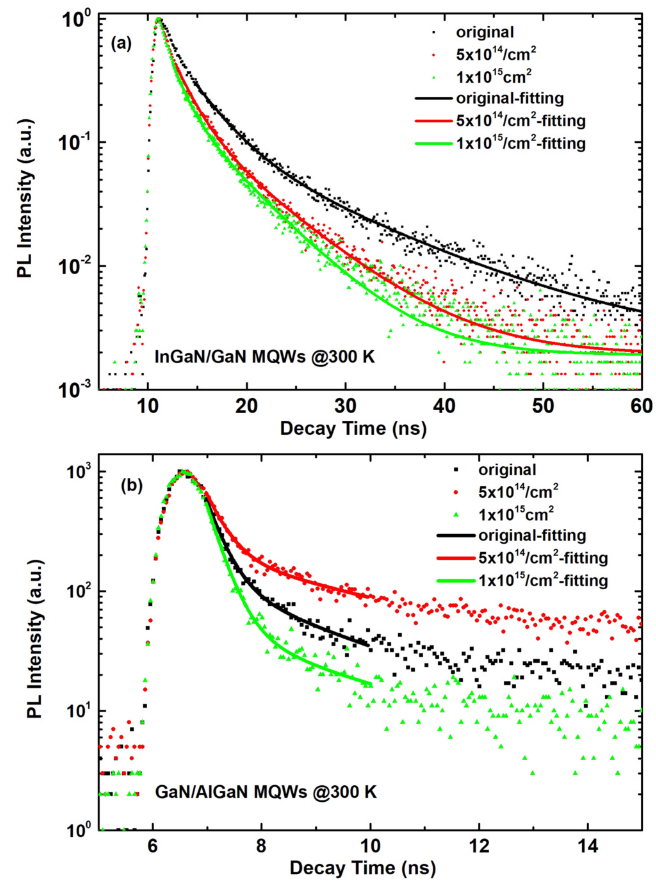

Fig. 6. Room temperature TRPL spectra and their double exponential fitting plots of (a) InGaN/GaN and (b) GaN/AlGaN MQWs with different electron fluence.

The TRPL decay curves of InGaN/GaN MQWs and GaN/AlGaN MQWs before and after irradiation at wavelengths of 458 nm and 365 nm, respectively, are shown in Fig. 6(a) and (b). The smooth solid lines without noisy signals are results of the fitting by double exponential curves described by the following formula [19]

$$I_{TRPL}(t) = A_1 exp\left(-\frac{t}{\tau_1}\right) + A_2 exp\left(-\frac{t}{\tau_2}\right) \tag{4}$$

where $I_{TRPL}(t)$ is decayed PL intensity at time of t, τ_1 and τ_2 are the faster and slower decay time, respectively. A_1 and A_2 are the fitting components, corresponding to τ_1 and τ_2. At room temperature, non-radiative recombination process is much faster than radiative process so that τ_1 (the smaller one) can represent the non-radiative recombination lifetime τ_{nr} in MQWs [20,21]. All the values of τ_{nr} in InGaN/GaN MQWs and GaN/AlGaN MQWs before and after electron irradiation are listed in Table 7.

Table 7
Non-radiative Recombination Lifetime τ_{nr} in MQWs with Different Electron Fluence.

Fluence (e/cm^2)	Original	5×10^{14}	1×10^{15}
InGaN/GaN MQWs (ns)	2.081	1.351	1.111
GaN/AlGaN MQWs (ns)	0.292	0.335	0.279

The τ_{nr} in InGaN/GaN MQWs is much larger than that of GaN/AlGaN MQWs due to the high crystalline quality in the former than in the latter. Point defects are known to cause tremendous decrease of emission efficiency, or very short τ_{nr}. In the InGaN/GaN MQWs, the τ_{nr} decreased monotonically as the electron fluence increased, indicating that more carriers were consumed without contributing to the luminescence. Compared with the results in TDPL analysis, the new NRCs generated by electron beam irradiation are the main reasons for the rapid decline of carrier non-radiative recombination lifetime and the decrease of IQE. In the GaN/AlGaN MQWs, the τ_{nr} increased slightly when the sample exposed to an electron fluence of 5×10^{14} e/cm^2, then return to nearly initial value when fluence reached 5×10^{14} e/cm^2. The abnormal variation of the τ_{nr} after electron irradiation implied a higher irradiation tolerance of GaN/AlGaN MQWs. The variation of the τ_{nr} is caused by the combined effects of exciton localization and NRCs reductions in the GaN/AlGaN MQWs, which has been proved by the TDPL analysis.

At last, the irradiation damage coefficient, K, of InGaN/GaN and GaN/AlGaN MQWs is respectively derived by linear fittings of room temperature PL lifetimes as functions of electron beam fluence using the following relation [22,23]

$$\frac{\tau_0}{\tau} = 1+K\phi_e \tag{5}$$

where ϕ_e is the electron fluence, τ_0 and τ are the room temperature PL lifetimes of original MQWs and MQWs after irradiation with electron fluence of ϕ_e. Values of τ_1 obtained by TRPL are set to be the PL lifetimes here according to the electron fluence.

The K value of InGaN/GaN MQWs is 4.66×10^{-16} cm^2/e, meanwhile that of GaN/AlGaN MQWs is 4.45×10^{-17} cm^2/e. Therefore, the damage coefficient of GaN/AlGaN is about one order of magnitude less than InGaN/GaN MQWs, which also indicates the different irradiation damage mechanisms of InGaN-related and GaN-related MQWs.

4. Conclusions

In this paper, the 10 MeV electron beam irradiation effects on InGaN/GaN and GaN/AlGaN MQWs were investigated and compared. GaN/AlGaN MQWs showed better irradiative tolerance than InGaN/GaN MQWs. The degradation of light emission properties in InGaN/GaN after irradiation was mainly caused by the generation of point defects in the MQWs. On the other hand, the electron irradiation caused reduction in both exciton localization energy and NRC density in the GaN/AlGaN MQWs, which finally resulted in less variation after irradiation.

Acknowledgements

This work was supported by the National Key Research and Development Program of China (No. 2016YFB0400803), the National Natural Science Foundation of China (NSFC) (Nos. U1505253, 61804034), the Science and Technology Program of Guangdong (No. 2017A070701025), and Pearl River S&T Nova Program of Guangzhou (No. 201806010087).

References

[1] I.M. Pryce, D.D. Koleske, A.J. Fischer, H.A. Atwater, Plasmonic nanoparticle enhanced photocurrent in GaN/InGaN/GaN quantum well solar cells, Appl. Phys. Lett. 96 (2010) 153501.
[2] L. Sun, J. Chen, J. Li, H. Jiang, AlGaN solar-blind avalanche photodiodes with high multiplication gain, Appl. Phys. Lett. 97 (2010) 191103.
[3] B. Albrecht, S. Kopta, O. John, L. Kirste, R. Driad, K. Köhler, M. Walther, O. Ambacher, AlGaN ultraviolet A and ultraviolet C photo detectors with very high specific detectivity D*, Jpn. J. Appl. Phys. 52 (2013) 08JB28.
[4] J. Yang, D.G. Zhao, D.S. Jiang, P. Chen, J.J. Zhu, Z.S. Liu, L.C. Le, X.G. He, X.J. Li, H. Yang, Y.T. Zhang, G.T. Du, Photovoltaic response of InGaN/GaN multi-quantum well solar cells enhanced by inserting thin GaN cap layers, J. Alloy. Compd. 635 (2015) 82–86.
[5] M. Peng, X. Zheng, H. Wei, Y. He, M. Li, Y. An, P. Qiu, Y. Song, Electric-field driven photoluminescence probe of photoelectric conversion in InGaN-based photovoltaics, Opt. Express 26 (2018) A615–A625.
[6] P.R.E. Idris, A. Ajia, Yusin Pak, Ermek Belekov, Manuel A. Roldan, Nini Wei, R.W.M. Zhiqiang Liu, Iman S. Roqan, Generated carrier dynamics in V-pit-enhanced InGaN/GaN light-emitting diode, ACS Photonics 5 (2018) 820–826.
[7] P. Dong, J. Yan, Y. Zhang, J. Wang, C. Geng, H. Zheng, X. Wei, Q. Yan, J. Li, Optical properties of nanopillar AlGaN/GaN MQWs for ultraviolet light-emitting diodes, Opt. Express 22 (2014) A320–A327.
[8] S. Wang, W. Tian, F. Wu, J. Zhang, J.N. Dai, Z.H. Wu, Y.Y. Fang, Y. Tian, C.Q. Chen, Efficient optical coupling in AlGaN/GaN quantum well infrared photodetector via quasi-one-dimensional gold grating, Opt. Express 23 (2015) 8740–8748.
[9] M. Osinski, P. Perlin, H. Schone, A.H. Paxton, Effects of proton irradiation on AlGaN/InGaN/GaN green light emitting diodes, Electron. Lett. 33 (1997) 1252–1254.
[10] M. Ali, O. Svensk, Z. Zhen, S. Suihkonen, P.T. Törmä, H. Lipsanen, M. Sopanen, K. Hjort, J. Jensen, Reduced photoluminescence from InGaN/GaN multiple quantum well structures following 40 MeV iodine ion irradiation, Phys. B 404 (2009) 4925–4928.
[11] W.B. D, M.P. A, B.J. B, Displacement damage effects in AlGaN/GaN high electron mobility transistors, IEEE Trans. Nucl. Sci. 56 (2012) 3077–3080.
[12] Van Allen, J. A, Radiation belts around the earth, Sci. Am. 200 (1959) 39–46.
[13] L. Liu, L. Wang, D. Li, N. Liu, L. Li, W. Cao, W. Yang, C. Wan, W. Chen, W. Du, X. Hu, Z.C. Feng, Influence of indium composition in the prestrained InGaN interlayer on the strain relaxation of InGaN/GaN multiple quantum wells in laser diode structures, J. Appl. Phys. 109 (2011) 073106.
[14] J.S. Hwang, A. Gokarna, Y.-H. Cho, J.K. Son, S.N. Lee, T. Sakong, H.S. Paek, O.H. Nam, Y. Park, Direct comparison of optical characteristics of InGaN-based laser diode structures grown on pendeo epitaxial GaN and sapphire substrates, Appl. Phys. Lett. 90 (2007) 131908.
[15] Y. Sun, Y.-H. Cho, H.M. Kim, T.W. Kang, S.Y. Kwon, E. Yoon, Effect of growth interruption on optical properties of In-rich InGaN/GaN single quantum well structures, J. Appl. Phys. 100 (2006) 043520.
[16] L. Wang, N. Liu, L. Song, B. Li, Y. Liu, Y. Cui, B. Li, Z. Zheng, Z. Chen, Z. Gong, W. Zhao, X. Cao, Baoyi Wang, J. Luo, Z. Han, multiple angle analysis of 30-MeV silicon ion beam radiation effects on InGaN/GaN multiple quantum wells blue light-emitting diodes, IEEE Trans. Nucl. Sci. 65 (2018) 2784–2791.
[17] K. Ding, Y. Zeng, R. Duan, X. Wei, J. Wang, P. Ma, H. Lu, P. Cong, J. Li, Enhancement of exciton–phonon interaction in InGaN quantum wells induced by electron-beam irradiation, Jpn. J. Appl. Phys. 48 (2009) 021001.
[18] I. Brener, M. Olszakier, E. Cohen, E. Ehrenfreund, A. Ron, L. Pfeiffer, Particle localization and phonon sidebands in GaAs/$Al_xGa_{1-x}As$ multiple quantum wells, Phys. Rev. B 46 (1992) 7927–7930.
[19] L. Liu, L. Wang, N. Liu, W. Yang, D. Li, W. Chen, Z.C. Feng, Y.-C. Lee, I. Ferguson, X. Hu, Investigation of the light emission properties and carrier dynamics in dual-wavelength InGaN/GaN multiple-quantum well light emitting diodes, J. Appl. Phys. 112 (2012) 083101.
[20] Y. Kawakami, A. Kaneta, L. Su, Y. Zhu, K. Okamoto, M. Funato, A. Kikuchi, K. Kishino, Optical properties of InGaN/GaNnanopillars fabricated by postgrowth chemically assisted ion beam etching, J. Appl. Phys. 107 (2010) 023522.
[21] S.F. Chichibu, K. Hazu, Y. Ishikawa, M. Tashiro, H. Namita, S. Nagao, K. Fujito, A. Uedono, Time-resolved photoluminescence, positron annihilation, and $Al_{0.23}Ga_{0.77}N$/GaN heterostructure growth studies on low defect density polar and nonpolar freestanding GaN substrates grown by hydride vapor phase epitaxy, J. Appl. Phys. 111 (2012) 103518.
[22] B.H. Rose, C.E. Barnes, Proton damage effects on light emitting diodes, J. Appl. Phys. 53 (1982) 1772–1780.
[23] F. Gaudreau, C. Carlone, A. Houdayer, S.M. Khanna, Spectral properties of proton irradiated gallium nitride blue diodes, IEEE Trans. Nucl. Sci. 46 (2001) 1778–1784.